Geographic Variation and Episodic Evolution in an Ordovician Trilobite

Abstract. *A single lineage of the trilobite* Flexicalymene *shows two evolutionary "punctuated equilibria" within a 2-million-year, 1000-square-kilometer stratigraphic interval. The 2 × 10⁵-year-long "punctuation" may represent parapatric speciation. Commonness of depth-related clines before, during and after this event suggests that short-term adjustment to local conditions was important in long-term evolution.*

Many questions about evolution have gone unanswered because the ages and environments of fossils could not be measured accurately enough to reveal and distinguish the exact temporal and environmental trends in anatomy. In this study we analyze temporal and clinal variation in the pygidium of the trilobite *Flexicalymene* (Figs. 1 and 2) along a "fossil" marine depth gradient in a 2 × 10^6-year-long, 1000-km^2 interval of the Middle Ordovician Trenton Group in central New York. Cisne and Rabe (*1*, *2*) have described this sequence, the way chronologic relationships of strata have been determined in relation to altered volcanic ash (bentonite) layers, and the way environment has been measured through gradient analysis of fossil communities. Results on *Flexicalymene* include unprecedented information on these questions: Is evolutionary change episodic, as predicted by the "punctuated equilibrium" theory that evolutionary change is concentrated in allopatric speciation events (*3*, *4*)? Is an episode's duration consistent with the theory? How long does speciation take? How common are geographic clines? How do they change with time (*5*)? How important are they in evolution (*5*)?

Flexicalymene fossils are common in a certain range of water depth throughout the sequence (*6*). Only one basically continuous lineage is represented (*7*). As is common in species of trilobites and very primitive modern arthropods, the trilobite's abdominal segmentation, an expression of its pattern of segmental growth (*8*, *9*), is variable (Figs. 1 and 2). Two factors seem to be involved: variation in the clarity with which body segments are expressed as axial rings and pleurae on the pygidium, the abdomen's dorsal shell, and variation in the number of body segments themselves.

We counted numbers of axial rings in virtually all usable pygidia among more than 8400 *Flexicalymene* specimens from over 300 collections (*10*): 350 pygidia in

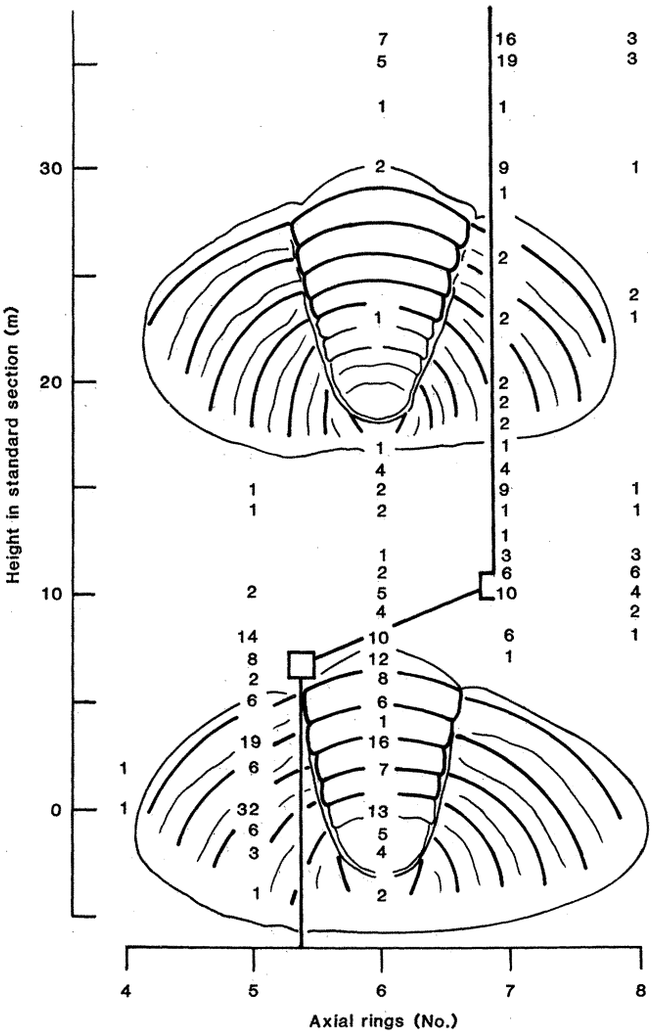

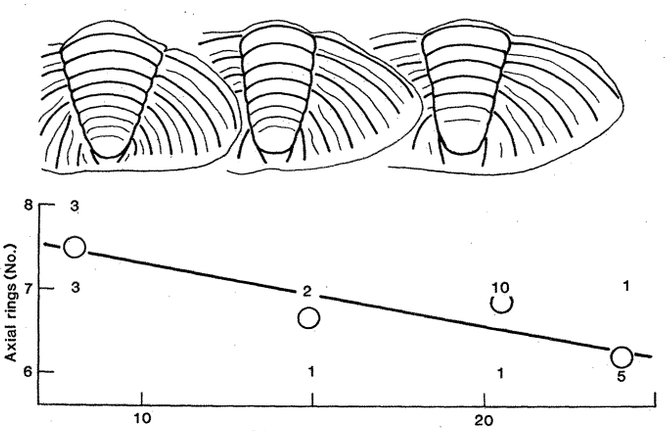

Fig. 1 (left). Evolution in *Flexicalymene*: temporal change in the number of axial rings (expressions of segments in the central, axial region) and pleurae (corresponding expressions in the paired lateral regions) in its pygidium. Camera lucida drawings show pygidia around 5 mm long with five axial rings and five pleurae (lower) and eight axial rings and six pleurae (upper). The spline curve (*18*) describes a "punctuated equilibrium" (*4*) in ring number. The punctuation (between the curve's join points; boxes indicate 95 percent confidence intervals for them) lasted a surprisingly long 2 × 10^5 years (*13*), a duration commonly associated with slower speciation (*3*, *25*). The event may signify parapatric speciation in conjunction with a cline like that in Fig. 2. Small numerals indicate numbers of specimens with the respective numbers of axial rings within standardized 1-m intervals (*13*). Fig. 2 (right). A "fossil" cline in *Flexicalymene*: depth-related change in the number of axial rings (expressions of segments in the central, axial region) and pleurae (corresponding expressions in the paired lateral regions) in its pygidium along a downslope transect (*16*) paralleling the altered volcanic ash bed in the 36th meter of the composite standard stratigraphic section (*13*). Camera lucida drawings show pygidia from this transect, each around 5 mm long, with eight axial rings and six pleurae (left), seven rings and six pleurae (middle), and six rings and five pleurae (right). The line fitted to average ring number by sampling station (circles) indicates the trend of the cline. Commonness of clines such as this throughout the 2 × 10^6-year-long stratigraphic sequence (*13*, *21*) indicates that directional anatomical change in fossils does not always represent evolution in the sense of change with time, and suggests that short-term adjustment to local conditions, as expressed in clines, can be important in long-term evolution. Small numerals indicate numbers of specimens with the respective numbers of rings for each sampling station.

0036-8075/80/0822-0925$00.50/0

101 collections from 19 stratigraphic sections along a 27-km downslope interval (data in Fig. 1). When possible, we counted numbers of pleurae and measured pygidial length (*11*). We analyzed the relation of axial ring number to the following variables (*12*): (i) pygidial length (*11*), (ii) time, as measured by height in a composite standard stratigraphic section (*13*), (iii) environment, as measured by reciprocal averaging ordination score for community samples (*14*), a measure that applies over the whole time span (*1, 2, 15*), and (iv) depth, as measured by position of samples on downslope transects along bentonite beds, an environmental measure that applies only within standardized 1-m time intervals (*1, 2, 13, 16*).

Corrected for the small influence of pygidial length (*12, 17*), ring number changes independently and significantly with both time (Fig. 1) and environment (Fig. 2), and time is the dominant factor (*17*). As shown in the spline curve (*18*) (Fig. 1), temporal change follows the "punctuated equilibrium" (*4*) pattern. The curve is consistent with the assumptions on which we fitted it: temporal change apparently has a definite, punctuational beginning and end between the curve's join points [6.7 ± 0.7 to 10.4 ± 0.8 m (95 percent confidence intervals); 6 to 11 m for analytic purposes] (*19*), and samples represent essentially the same environmental range over time (*20*). Thus, on the basis of the join points' separation, the "punctuation" evidently lasted roughly 2×10^5 years (*13*).

Clines in ring number (for example, Fig. 2) are frequent. Along six of nine transects (*16*), ring number changes consistently and significantly with at least one of the two environmental measures (*21*). Although clines occur before, during, and after the punctuation (*21*), grouped data indicate significant clinal variation only in the −4- to 5-m interval (*19*), suggesting that clines continually changed, on roughly a 10^5-year scale in such a way as to blur indications of clinal variation over longer periods. It is unlikely that postmortem transport of remains substantially affected evidence of clines (*1, 2*).

Temporal and clinal trends probably represent change in the genetic makeup of a population (*6, 7*). Temporal constancy of ring number at different values but across the same environmental range before and after the punctuation (*19, 20*) (Fig. 1) strongly suggests genetic inheritance of ring number. As different manifestations of the same anatomical phenomenon, temporal and clinal variation probably had the same basis, most likely genes controlling segmental growth.

That *Flexicalymene* shows clinal variation at all is surprising. Its protaspis larva [figure 19 in (*8*)] was early-hatching and probably dispersal-adapted. Modern marine invertebrates with such larvae typically show very slight geographic variation over much greater distances (*5*, p. 25; *22*). For *Flexicalymene*, as for the associated trilobite *Triarthrus* (*23*), development of clines was probably related to the unusually strong gradient in depth-related environmental conditions.

Flexicalymene offers much of potential interest as regards evolutionary and biostratigraphic theory:

1) Although it has traditionally been equated with strictly temporal evolutionary change, directional anatomical variation can have an unexpectedly strong clinal component even in a local area.

2) Short-term adjustment to local environmental conditions, as expressed in clines, can be important in evolution over the long term (*5*).

3) Although *Flexicalymene* shows punctuated equilibria (Fig. 1), the "punctuated equilibrium model" (*3, 4*) may not account for them. The punctuation's duration is orders of magnitude longer than would be expected for ecological displacement of one species by another (*3, 24*).

4) The punctuation may represent parapatric speciation. Its duration is about that expected for slower speciation modes (*3, 25*). The presence of only one lineage (*6, 7*), the commonness of clines (*21*), and the similarity between temporal and clinal trends (Figs. 1 and 2) suggest that, if the event represents speciation at all, speciation was of this type. In this case, the punctuation would represent a hybrid zone developed over a much larger region as it formed and broke down in one small area (*5*).

5) If in fact evolutionary equilibrium is an appropriate concept, temporal equilibrium was attained before and after the punctuation even though spatial equilibrium, in the sense of long-lasting zero clinal variation, never was.

JOHN L. CISNE
Department of Geological Sciences and
Division of Biological Sciences,
Cornell University,
Ithaca, New York 14853
GEORGE O. CHANDLEE
BRUCE D. RABE
Department of Geological Sciences,
Cornell University
JILL A. COHEN
Department of Agronomy,
Cornell University

References and Notes

1. J. L. Cisne and B. D. Rabe, *Lethaia* **11**, 341 (1978).
2. B. D. Rabe and J. L. Cisne, *ibid.* **13**, 109 (1980).
3. E. Mayr, *Populations, Species, and Evolution* (Belknap, Cambridge, Mass. 1970), pp. 266, 296–350.
4. N. Eldredge and S. J. Gould, in *Models in Paleobiology*, T. J. M. Schopf, Ed. (Freeman, San Francisco, 1972), pp. 82–115; S. J. Gould and N. Eldredge, *Paleobiology* **3**, 115 (1977).
5. J. A. Endler, *Geographic Variation, Speciation, and Clines* (Princeton Univ. Press, Princeton, N.J., 1977).
6. For diagrams of the trilobite's stratigraphic distribution, see figures 4 and 5 in (*1*) and figures 2 and 3 in (*2*).
7. Only one *Flexicalymene* lineage, *F. senaria* (Conrad), is known in these long and intensively studied strata. One and the same ecological type appears to have been present before, during, and after the punctuation (*6, 18*). Whether *F. senaria* represents one or more biological species is impossible to determine, though only one seems to have been present at any one time.
8. H. B. Whittington, *Biol. Rev.* **32**, 421 (1957).
9. J. L. Cisne, *Foss. Strata* **4**, 45 (1975).
10. Cisne and Rabe (*1*) describe the sampling procedure. Almost all pygidia analyzed represent adults. The few smallest probably represent late juveniles.
11. Pygidial length (L) was measured between the front of the most anterior axial ring and the pygidium's posterior margin by means of a dissecting microscope's ocular reticle.
12. The choice of analytic methods and the precision of statistical inference are limited in that ring number takes so few discrete values. Since ring number (A) is highly correlated with pygidial length (L) (*11*), time (T) (*13*), and environment (E) (*15*) and time-specific depth (D) (*16*), partial correlation coefficients have been used to assess the relation of ring number to time ($r_{AT.LE}$) and to environment ($r_{AE.LT}$, $r_{AD.L}$) while adjusting for the influences of other factors. Significance levels quoted are those that would apply for two-tailed tests given normal distribution of ring number. They should be understood as approximations.
13. Time (T) is measured in terms of standardized 1-m increments that, according to Fisher's [*N.Y. State Mus. Sci. Serv. Map Chart Ser. No. 25* (1977)] correlation chart, have an average duration of about 5×10^4 years; see (*1*).
14. M. O. Hill, *J. Ecol.* **61**, 237 (1973); *J. R. Stat. Soc. Ser. C* **23**, 340 (1974). With the use of DECORANA (Cornell Ecology Programs CEP-40), 286 community samples were ordinated on the basis of the relative abundances of macroinvertebrate genera (*10*). First axis scores (0 to 100 scale) are used here.
15. The logarithm of reciprocal averaging score (E) (*14*) increases approximately linearly with distance downslope along each of nine downslope transects along bentonite beds; see (*1*).
16. Although depth changed over longer periods, distance downslope (D) on a transect measures relative depth within the standardized 1-m interval (*13*) containing the particular bentonite bed (*1, 2*). Pygidia studied cover 9- to 23-km downslope intervals on transects in the 0th, 2nd, 3rd, 8th, 11th, 14th, 15th, 35th, and 36th meters.
17. Ring number is significantly ($P < .001$; $N = 349$) correlated with both time ($r_{AT.LE} = 0.60$) and environment ($r_{AE.LT} = 0.24$) (*12*). Coefficients for the regression of sample-averaged ring number on the corresponding, standardized (zero mean, unit variance) variables show the factors' approximate (*12*) relative importance: time (T) has nearly three times the impact of environment (E), and more than 50 times the impact of sample-averaged pygidial length (L).
18. Fitted by the Gauss-Newton method by means of *SAS* (Statistical Analysis System; SAS Institute, Raleigh, N.C.), the spline curve (Fig. 1) satisfactorily explains the data on the constancy-change-constancy punctuated equilibrium model (convergence criterion met; residual sum of squares/corrected total sum of squares = 0.47). Trials with several initial locations of the join point by this and other methods confirm that the solution given represents the only satisfactory one.
19. For the −4- to 5-, 6- to 11-, and 12- to 36-m intervals, $r_{AT.LE}$ (*12*) indicates significant ($P < .1$) correlation between ring number and time only in the 6- to 11-m interval ($P < .001$); $r_{AE.LT}$ (*12*) indicates significant $P < .1$) correlation with environment only in the −4- to 5-m interval ($P < .05$).
20. At the .05 level, the distribution of E value (*15*)

does not differ significantly from the normal in the 6- to 11- and 12- to 36-m intervals, and differs from it in the −4- to 5-m interval only on account of one sample's low score, according to Filliben's [*Technometrics* **17**, 111 (1975)] test. The distributions' means do not differ even at the .4 level. Only the 12- to 36-m distribution differs from others in variance, having a slightly but, at the .05 level, significantly higher one.
21. For the nine transects (*16*), $r_{AD.L}$ (*12*) indicates significant ($P < .1$) clinal variation in the 3rd and 36th ($P < .001$), 15th ($P < .01$), and possibly 2nd and 8th ($P < .1$) meters; $r_{AE.L}$ (*12*) indicates significant clinal variation in the 2nd, 8th, and 14th ($P < .05$), 36th ($P < .001$), and possibly 15th ($P < .1$) meters. Discrepancies as to indications of clines between the two environmental measures (*D* and *E*) (*15*, *16*) likely are due to a small number of specimens per transect, and possibly to changes in environment or clines within meter intervals. Results are indeterminate ($.1 < P < .9$) as to clines along other transects (*16*).
22. S. Ekman, *Zoogeography of the Sea* (Sidgwick & Jackson, London, 1953), pp. 244–263.
23. J. L. Cisne, J. Molenock, B. D. Rabe, *Lethaia* **13**, 47 (1980).
24. C. S. Elton, *The Ecology of Invasions by Animals and Plants* (Chapman and Hall, London, 1958), pp. 117–124; also see (*5*), pp. 152–178.
25. D. J. Futuyma, *Evolutionary Biology* (Sinauer, Sunderland, Mass., 1979), pp. 424–426.
26. We thank B. Grimes and D. J. Solomon, who helped with statistical analyses, and W. L. Brown, Jr., J. E. Oliver, R. J. Ross, Jr., F. H. T. Rhodes, J. W. Wells, and anonymous reviewers for constructive criticism. Supported by NSF grants DEB-7509651 and DEB-7803179.

4 January 1980; revised 15 May 1980

Binding and Factor XIII$_a$–Mediated Cross-Linking of a 27-Kilodalton Fragment of Fibronectin to *Staphylococcus aureus*

Abstract. *A 27-kilodalton tryptic fragment, derived from the amino terminus of the 200-kilodalton fibronectin subunit, inhibited binding of intact fibronectin to* Staphylococcus aureus *and could be cross-linked to* Staphylococcus aureus *by blood coagulation Factor XIII$_a$. Interactions of fibronectin with* Staphylococcus aureus *via this fragment may be important for bacterial opsonization and attachment.*

Fibronectin is a high-molecular-weight glycoprotein that is found in a soluble form in blood and other body fluids; it is found in an insoluble form in connective tissues and is associated with basement membranes (*1*). In cell culture, fibronectin is secreted into the media of cultured adherent cells and is organized into an extracellular fibrillar matrix (*2*). Transformed cells generally lack a fibronectin matrix (*1*). Fibronectin binds to *Staphylococcus aureus* (*3*) and opsonizes this organism for neutrophils (*4*). Fibronectin also binds to collagen, sulfated proteoglycans, hyaluronic acid, fibrin, and gangliosides and is a substrate for blood coagulation Factor XIII$_a$ (plasma transglutaminase) (*1*). As a result of these multiple interactions, fibronectin probably functions as an adhesive and opsonic protein (*1*).

Thrombin (*5*, *6*), plasmin (*7*), and low concentrations of trypsin (*6*) cleave the 200-kilodalton (kd) subunit of human plasma fibronectin into 27-kd and 160- to 180-kd fragments. The 27-kd fragment contains the site or sites of Factor XIII$_a$ transamidation (*6*, *7*) and mediates cross-linking to collagen (*6*). The 160- to 180-kd fragments contain separate sites that mediate binding to collagen (*5*, *6*, *8*), heparin (*9*), and eukaryotic cells (*10*). Sequence analysis places the 27-kd fragment at the NH_2-terminus and the 160- to 180-kd fragments toward the COOH-terminus of the 200-kd fibronectin subunit (*5*). We now report that the binding site for *S. aureus* is in the 27-kd fragment and that both intact fibronectin and the 27-kd fragment can be cross-linked to *S. aureus* by Factor XIII$_a$.

Two-dimensional electrophoretic analysis [isoelectric focusing followed by discontinuous slab polyacrylamide gel electrophoresis in the presence of sodium dodecyl sulfate (*11*)] revealed that the 27-kd fragment of early tryptic digests is the only sizable basic fragment in either early or late tryptic digests of fibronectin; the other fragments are acidic. Therefore, chromatography of the early tryptic digest on diethylaminoethyl (DEAE)-cellulose efficiently separated the 27-kd fragment from 160- to 180-kd fragments and traces of a 31-kd fragment (Fig. 1). The 27-kd fragment could be distinguished from the 31-kd fragment by three criteria in addition to migration in gels: (i) the 27-kd fragment contained the

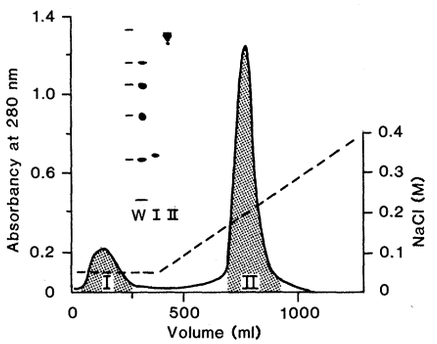

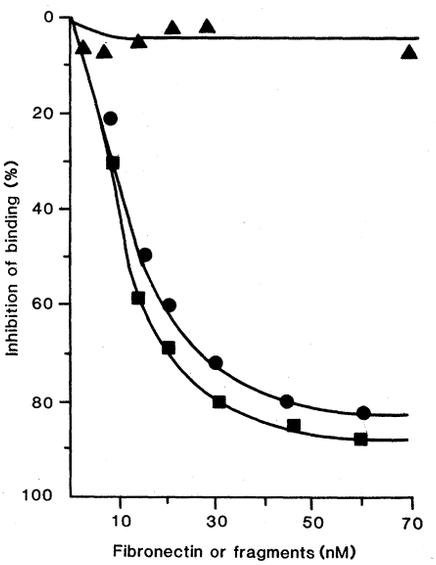

Fig. 1 (left). Chromatographic separation of fragments of lightly trypsinized fibronectin. Plasma fibronectin was purified from a fibrinogen- and fibronectin-rich side fraction of Factor VIII preparation (*6*). The purified protein (6.4 mg/ml) was incubated in tris-buffered saline, *p*H 7.4, with trypsin (1 μg/ml) at 37°C. After 15 minutes, soybean trypsin inhibitor (5 μg/ml) was added. The mixture was diluted threefold with water and applied to a column (5 by 6 cm) of DEAE-cellulose, equilibrated and eluted with a buffer of 0.01*M* tris-chloride and 0.05*M* sodium chloride (*p*H 7.4). The pass-through peak, I, contained the 27-kd fragment (inset). The 160- to 180-kd fragments, along with traces of a 31-kd fragment, were eluted in peak II by a 1-liter, linear (0.05*M* to 0.40*M* sodium chloride) gradient. The fractions were concentrated by precipitation with 90 percent saturated ammonium sulfate, dissolved in and dialyzed against tris-buffered saline, and stored at −70°C. Peak fractions were analyzed after reduction by discontinuous slab polyacrylamide gel electrophoresis (inset). The migration of the fragments was compared to the migration of size standards (*W*): (from top to bottom) fibronectin, 200 kd; phosphorylase, 93 kd; albumin, 68 kd; ovalbumin, 43 kd; and chymotrypsinogen, 24.5 kd. Fig. 2 (right). Inhibition of binding of ^{125}I-fibronectin to *S. aureus* by fibronectin fragments. Varying concentrations of 27-kd or 160- to 180-kd fibronectin fragments or intact fibronectin were incubated for 2 hours at 22°C with lyophilized *S. aureus* (0.4 mg/ml; approximately 0.8×10^8 bacteria per milliliter) in tris-buffered saline (*p*H 7.4) containing 0.1 percent albumin. ^{125}I-Labeled fibronectin (3 n*M*) was added, the mixtures were incubated for an additional 2 hours at 22°C, and bound and unbound ^{125}I-labeled fibronectin were separated by centrifugation ($10^4 g$ for 2.5 minutes) in a Microfuge. The labeling in both the supernatant and the top of the Microfuge tube, which contained the bacteria, was determined in a gamma counter. In the absence of unlabeled fibronectin or the 27-kd fragment, 10 percent of the ^{125}I-labeled fibronectin bound to the bacteria. Concentrations of intact fibronectin and fibronectin fragments were calculated from absorbance of 280 nm, based on the extinction coefficient of intact fibronectin (*16*). (●) Intact fibronectin; (■) 27-kd fragment; and (▲) 160- to 180-kd fragments.

0036-8075/80/0822-0927$00.50/0